

Repeated fracture and healing of silicic magma generate flow banding and earthquakes?

Hugh Tuffen

Donald B. Dingwell

Harry Pinkerton

Department of Earth and Environmental Sciences, University of Munich, Theresienstraße 41, D-80333 Munich, Germany

Department of Environmental Science, Lancaster University, Lancaster LA1 4YQ, UK

ABSTRACT

Textures in an exceptionally preserved effusive rhyolite conduit at Torfajökull, Iceland, indicate that rising magma repeatedly fractured and healed at shallow levels in the conduit (RFH process). Anastomosing tuffisite veins filled by fine-grained juvenile clasts were generated by shear fracture of highly viscous magma in the glass transition interval. Welding of the particulate material during subsequent deformation led to thorough healing of veins, allowing repeated fracture of the same body of magma. We propose that the RFH process is a rechargeable trigger mechanism for hybrid seismicity and show that the time scale of the process and the fractures formed by it are consistent with the repeat time and magnitude of hybrid earthquakes during silicic eruptions. The RFH process may also form the flow banding that is nearly ubiquitous in obsidian.

Keywords: volcanic earthquakes, obsidian, tuffisite, viscoelasticity, glass transition, conduit.

INTRODUCTION

The eruption of silicic lava domes is typically accompanied by repetitive long-period and hybrid earthquakes that originate from a small region of the upper conduit, typically <1.5 km from the dome surface (Chouet, 1996; Neuberg, 2000). Both hybrid and long-period earthquakes are small magnitude ($M_0 \sim 0-1$) and contain similar frequencies, but hybrid events have mixed-polarity first motions, whereas long-period first motions are single polarity (Lahr et al., 1994). Repeat times between successive long-period and hybrid events are typically minutes to hours ($10^{2.5}$ to $10^{4.5}$ s) (Gil Cruz and Chouet, 1997; White et al., 1998; Voight et al., 1999; Uchida and Sakai, 2002). Although increased numbers of hybrid and long-period earthquakes may occur prior to, and thus give advance warning of, dome collapse and Vulcanian explosions (Chouet, 1996; Voight et al., 1999; Neuberg, 2000), their origins are controversial. Long-period earthquakes may be triggered when gas released by foam collapse excites preexisting cracks in the dome and conduit (Gil Cruz and Chouet, 1997), or by magma-water interaction (Neuberg, 2000), whereas hybrid earthquakes may be triggered by shear fracture, stick-slip motion, or hydraulic fracturing (Goto, 1998; White et al., 1998; Neuberg, 2000; Uchida and Sakai, 2002). To date, no trigger model has drawn on the geologic evidence preserved at ancient, dissected conduits for processes that occur at shallow levels during magma ascent. We describe textures at a rhyolitic conduit in Iceland that point toward repeated shear fracture and welding of magma as a rechargeable trigger mechanism for hybrid earthquakes. Simple fracture-welding models and the nature of the

fractures formed are used to argue that the process is consistent with the characteristics of hybrid earthquakes worldwide.

RHYOLITIC CONDUIT AT TORFAJÖKULL

Partial flank collapse of southeast Rauðufossafjöll, a ca. 60 ka subglacial rhyolite tuya at Torfajökull, Iceland, has exposed a 10-m-wide dike-like conduit (Fig. 1) 20–30 m beneath the subaerial peralkaline rhyolite lava flow that it fed (Tuffen, 2001; Tuffen et al., 2003). The 10^6 m³ lava flow represented the final effusive phase of an initially explosive eruption. Multiple generations of angular, anastomosing tuffisite veins 1–60 mm wide and ranging from tens of centimeters to >1 m in length cut the vesicle-free, microlite-free, dark gray obsidian of the conduit margins (Fig. 1D). Veins are filled by densely welded pale gray clastic material (fragments of magma and broken phenocrysts); the clasts are mostly 10–200 μ m across (Fig. 2A), and they are disposed in complex sedimentary structures, including planar bedding and cross-bedding (Fig. 2B). Clasts are of varying grain size and sorting and make up commonly folded and deformed beds ranging from <0.1 mm to 10 mm in thickness. Beds containing the finest-grained material are locally adjacent to vein walls (Fig. 2B). Viscous deformation of juvenile clasts, with shear strain between 1 and 10, has removed all pore space in the vein-filling material (Fig. 2A). It has led to a pervasive foliation (eutaxitic texture), which overprints bedding orientations and is commonly crenulated. Locally, vein walls are cut by microfractures and are adjacent to trains of smaller particles that they appear to have shed (Fig. 2C).

Earlier veins have undergone viscous deformation parallel to the magma flow direction and appear as elongate, often crenulated mid-gray bands that are progressively rotated toward vertical with increasing strain (Fig. 2D). They are locally cut by less-deformed veins. Axial strain is typically 2–10 in deformed veins and generally increases toward the center of the conduit. Relict bedding is distinguishable in less-deformed veins, whereas the most-deformed veins appear as bands of subtly paler color than the surrounding obsidian.

INTERPRETATION OF TEXTURES

The tuffisite veins are interpreted as shear fractures formed by the non-Newtonian response of highly viscous magma to flow-related strain in the conduit (Goto, 1998). The fine-grained material produced during shear on fracture planes (Fig. 2C; Sparks et al., 2000; Schwarzkopf et al., 2002) was redeposited by flow of a gas-particle mixture through the fracture system (Heiken et al., 1988; Stasiuk et al., 1996). The gas phase was probably derived from vesicular magma rising in the conduit center (Heiken et al., 1988; Stasiuk et al., 1996). Gas accumulation in the center may have increased strain rates and shear stress in the conduit margins, leading to fracture (Uchida and Sakai, 2002).

Ductile deformation of veins indicates that magma underwent solid-like and fluid-like deformation on different time scales (Dingwell, 1996; Sparks, 1997; Marti et al., 1999). Welding of vein-filling material allowed such thorough healing that magma regained mechanical isotropy, and later fractures cut earlier ones. This process contrasts with cataclastic shear zones on surfaces of spines at the Montserrat lava dome, which never completely heal (Sparks et al., 2000). The magma at Torfajökull could heal more efficiently because of its lower crystallinity (<15% as opposed to >90% at Montserrat). Progressive deformation and rotation of earlier veins during magma flow have created flow bands of distinctive glass color and crystal sizes. Such bands are nearly ubiquitous in obsidian (e.g., Smith, 2002; Rust et al., 2003).

Together, the textures are thought to record repeated fracture and healing of rising magma (RFH process).

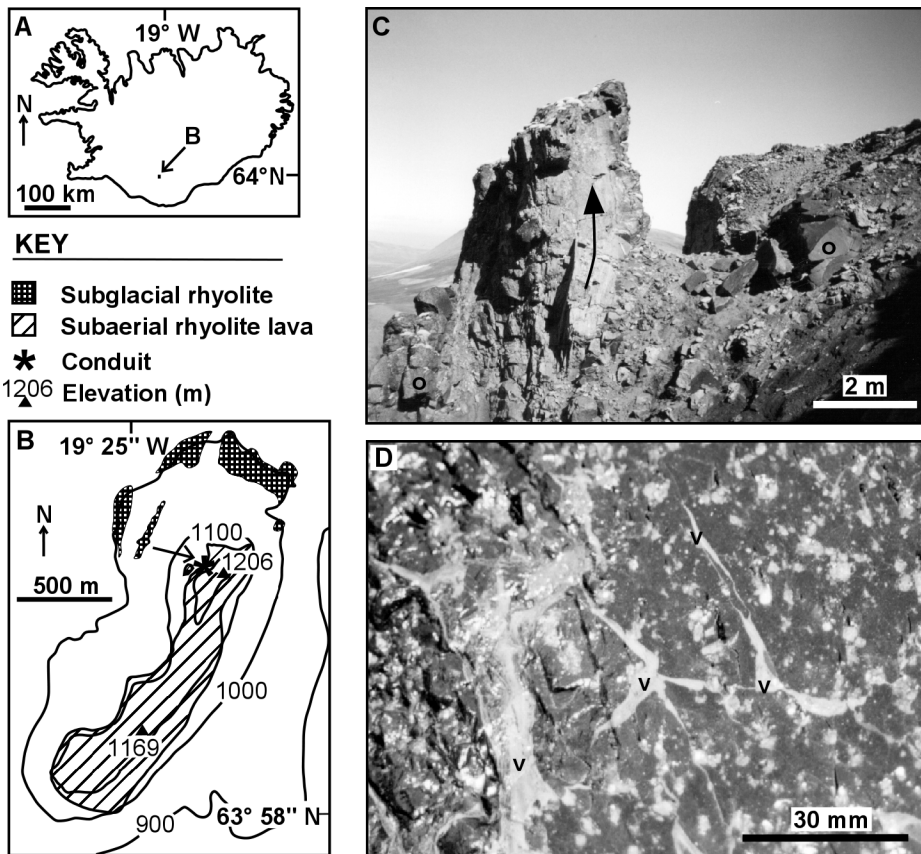


Figure 1. Location and photographs of conduit. **A:** Location of southeast Rauðufossafjöll in south-central Iceland. **B:** Geologic map of southeast Rauðufossafjöll, simplified from Tuffen et al. (2003), showing location of conduit. **C:** Overview of conduit, showing dark gray obsidian walls (o) and near-vertical flow banding in devitrified interior (arrow). **D:** Network of angular, branching, pale gray tuffisite veins (v) in conduit-wall obsidian. Pale blobs are feldspar phenocrysts.

VEIN FORMATION AS A TRIGGER FOR HYBRID EARTHQUAKES?

We propose that the RFH process is a trigger mechanism for hybrid earthquakes and support the proposal with the following lines of evidence: (1) Veins record repeated fracture of a small body of magma (RFH process) and thus point to a rechargeable trigger mechanism (Neuberg, 2000). (2) Sedimentary structures in veins record flow of a gas-ash mixture through a crack, a process that may generate seismic signals (Chouet, 1988, 1996). (3) The dimensions of tuffisite veins described here are similar to the “precursor crack” inferred to have been excited during long-period seismicity at Galeras (Gil Cruz and Chouet, 1997). Since there is little difference in the frequency content of hybrid and long-period events (Lahr et al., 1994), fractures associated with hybrid events are likely to have similar dimensions. (4) The grain size of vein-filling material (10–200 μm) is compatible with estimates of particle size from fluid-driven crack models (Kumagai and Chouet, 1997). (5) Fracture events are likely to generate earthquakes of a magnitude similar to that of recorded hybrid and long-period events. The seismic moment M_0 associated with tuffisite

vein formation is calculated to be $10^{8.5}$ N·m on the basis of the equation $M_0 = DGA$ (Shearer, 1999) and reasonable estimates of mean displacement D (~ 10 mm), shear modulus G ($\sim 10^{10}$ Pa), and fault area A (~ 3 m²). This seismic moment equates to a moment magnitude of roughly -1 , similar to hybrid and long-period events at Satsuma-Iojima, Galeras, and Unzen (Umakoshi et al., 1993; Gil Cruz and Chouet, 1997; Uchida and Sakai, 2002).

However, it is necessary to determine whether the time scale of the RFH process is also consistent with observed repeat times of hybrid and long-period earthquakes during eruptions.

TIME SCALE OF RFH PROCESS Strain Rate–Induced Fracture of Viscoelastic Magma

Our model of the RFH process involves (1) shear-stress accumulation during viscoelastic deformation, (2) stress release by brittle fracture, and (3) subsequent healing and relaxation of magma, allowing stress reaccumulation and a repeat of the process. In order to estimate the cycle time between successive fracture events (Gomberg, 2001), we first estimate

the time taken for accumulating stress to cause fracture.

Unrelaxed magma deformation, which allows accumulation of shear stresses during flow, occurs when the product of strain rate and shear viscosity exceeds 10^7 Pa (Webb and Dingwell, 1990). Linear viscoelastic deformation, which occurs when strain rate times viscosity is 10^7 to 10^{10} Pa (Webb and Dingwell, 1990), obeys Maxwell’s equation (Maxwell, 1867):

$$\sigma_s + \frac{\eta_s}{G} \frac{\partial \sigma_s}{\partial t} = \dot{\epsilon} \eta_s, \quad (1)$$

where σ_s is shear stress, η_s is shear viscosity, G is shear modulus ($\sim 10^{10}$ Pa; Webb and Dingwell, 1990), t is time, and $\dot{\epsilon}$ is shear-strain rate. If we apply the initial condition that $\sigma_s = 0$ at $t = 0$ and we assume a constant strain rate, solving equation 1 to give shear stress as a function of time yields

$$\sigma_{st} = \dot{\epsilon} \eta_s (1 - e^{-tG/\eta_s}). \quad (2)$$

Fracture will occur if shear stress exceeds shear strength τ_s , at time t_f given by

$$t_f = -\frac{\eta_s}{G} \ln(1 - \tau_s/\dot{\epsilon} \eta_s), \quad (3)$$

obtained by rearranging equation 2. Analysis of equations 2 and 3 shows that fracture will only occur if $\dot{\epsilon} \eta_s > \tau_s$, which demonstrates that fracture is not an inevitable consequence of non-Newtonian deformation—an assumption implicit in existing models of strain-induced fracture (Goto, 1998; Papale, 1999). However, because $\dot{\epsilon} \eta_s$ must exceed 10^7 Pa for viscoelastic deformation to occur and because the shear strength of natural magma is typically 10^6 to 10^7 Pa (Romano et al., 1996; Voight et al., 1999), fracture is likely to accompany viscoelasticity. Magma strengths of 10^6 and 10^7 Pa are considered in this paper.

Next we estimate the strain rate in conduits during effusive silicic eruptions. The highest strain rate during Newtonian flow of uniformly viscous magma in a cylindrical conduit occurs at the walls and is given by $4Q/\pi r^3$, where Q is magma flux (in m³·s⁻¹) and r is conduit radius (in m) (Goto, 1998). This is only a rough approximation of true strain-rate maxima, because cooling and degassing will create a viscosity gradient (Wylie et al., 1999) and flow will become non-Newtonian. Vesicle morphologies in conduit wall–derived obsidian from the Rock Mesa pyroclastic deposit, Oregon, indicate a strain rate of 10^{-2} s⁻¹ (Rust et al., 2003). By comparison, values of magma-discharge rate and conduit diameter from recent dome-building eruptions at Montserrat (Voight et al., 1999), Unzen (Goto,

1998), and Merapi (Hammer et al., 2000) provide Newtonian strain-rate maxima between $10^{-2.5}$ and 10^{-6} s^{-1} . Thus, a plausible range of strain rates is 10^{-2} to 10^{-6} s^{-1} .

Healing of Fractures by Welding

Welding in tuffsite veins is likely to be far more rapid than welding in pyroclastic flow deposits (e.g., Sparks et al., 1999), because the welded material undergoes negligible cooling and is isolated from insoluble atmospheric gases. Welding involves a diffusion-related process (sintering), in which cohesion between surfaces of adjacent particles is established (Sparks et al., 1999; Gottsmann and Dingwell, 2002), and viscous deformation, in which pore space between imperfectly packed particles is removed (Sparks et al., 1999). The rate of the diffusion-related process t_d may be roughly approximated by the relaxation time (Gottsmann and Dingwell, 2001), hence $t_d = \eta_s/G$. Tuffsite textures indicate that viscous strain of ~ 1 in the glass particles was sufficient to remove porosity (Fig. 1D). The time scale for viscous deformation, t_v , is therefore given by $1/\dot{\epsilon}$, the time for a shear strain of 1.

The total time T_t for each RFH cycle is the sum of the fracture time and the welding time, $T_t = t_f + t_d + t_v$, and is shown in Figure 3 as a function of magma viscosity.

Total Cycle Time and Magma Viscosity

Assuming that each fracture event during the RFH process triggers a seismic signal, and only one fracture forms at a time, the repeat time of seismic signals is equal to T_t . At the reasonable values of strain rate and magma strength already given, T_t is similar to the repeat times of recorded hybrid and long-period events when magma viscosity is in the range 10^9 – 10^{14} Pa·s (Fig. 3). This corresponds well to the range of viscosities extant in super-cooled liquid magma within the glass transition interval (Gottsmann et al., 2002). Experiments indicate that this viscosity range translates to a temperature range of 136 K in basalt and 211 K in pantellerite (Gottsmann et al., 2002). RFH behavior may only occur if magma reaches this temperature range without completely crystallizing, because welding requires a melt phase. The minimum cooling rate necessary to avoid crystallization depends upon magma composition and is indicated by the slowest cooling rates measured by relaxation geospeedometry on natural glassy samples. Basalt crystallizes rapidly and must be cooled at least 0.1 K/s (Wilding et al., 2000), whereas pantellerite crystallizes more slowly and may be cooled as slowly as 10^{-5} K/s (Gottsmann and Dingwell, 2002). At these cooling rates, basalt could dwell only 10^3 s in the viscosity range 10^9 – 10^{14} Pa·s, insufficient for multiple cycles, whereas the corresponding time for pantellerite, 10^7 s, permits many cy-

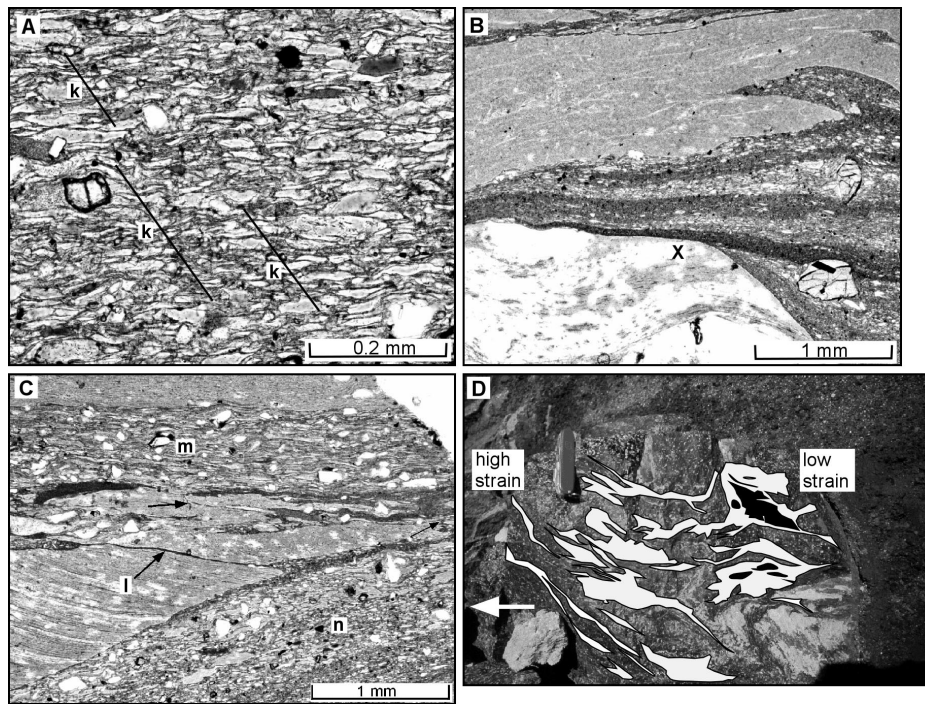


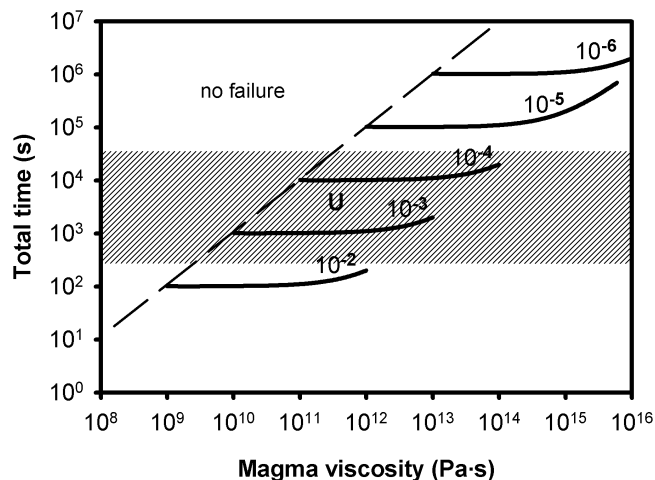
Figure 2. Textures in tuffsite veins. A: Photomicrograph of eutaxitic texture in densely welded tuffsite. Shear strain of ~ 1 in pale gray glassy fragments has removed all pore space. Subtle kink bands (k) in foliation cross boundaries between adjacent fragments, indicating that cohesive deformation of welded material occurred (Marti et al., 1999), rather than cataclastic flow (Sparks et al., 2000). B: Photomicrograph of bedded tuffsite vein (center). Fine-grained bed (dark) is adjacent to vein wall (pale gray, bottom) at X. Presence of finest-grained material on fracture surfaces demonstrates that local clastic redeposition occurred. In situ cataclasis may also generate “bedding,” but coarsest-grained material is likely to occur on fracture surfaces (Schwarzkopf et al., 2002). C: Photomicrograph of obsidian wall (l) between two vein branches (m, n), which is cut by small shear fractures (arrows). This process appears to have generated much of fragmental material during opening and deformation of veins. Note high strain in vein branch m and low strain in branch n in plane of thin section. D: Tuffsite veins are increasingly deformed and rotated toward center of conduit (arrow). Veins overdrawn for clarity; penknife is 7 cm long. Modified from Tuffen (2001).

cles of fracture and welding. RFH behavior may thus be a characteristic feature of silicic magma compositions only.

In contrast with the conduit described here, significant microlite crystallization occurs at andesitic-dacitic lava domes such as Montserrat and Unzen and leads to increased viscosity

and pressurization of magma (Sparks, 1997; Voight et al., 1999). It may also lead to RFH behavior, because (1) tuffsite veins occur at Montserrat and other domes (Sparks, 1997), (2) measured magma viscosities also fall within the 10^9 – 10^{14} Pa·s range (Goto, 1998; Voight et al., 1999; Sparks et al., 2000), and

Figure 3. Calculated total time T_t for each RFH (repeated fracture and healing) cycle during conduit flow. Curves are for different strain rates, indicated in units of s^{-1} . No fracture occurs to left of dashed line. Shaded area indicates repeat time of hybrid and long-period earthquakes during recent silicic dome eruptions (Gil Cruz and Chouet, 1997; Voight et al., 1999). Magma viscosities of 10^9 – 10^{14} Pa·s give total times consistent with these observations. U indicates inferred viscosity and strain rate of magma undergoing shear fracture at Unzen (Goto, 1998).



(3) there is textural evidence for mixed ductile-brittle deformation within highly crystalline domes (Smith et al., 2001). Pressurization may provoke fracture by increasing strain rates, and magma far from the dome surface may retain sufficient melt to heal (cf. Sparks et al., 2000).

The RFH process may occur anywhere in the conduit where the magma viscosity and strain rate are sufficiently high. Regions of the conduit where heat flux through the walls is high (e.g., because of hydrothermal circulation) would be especially prone to fracture, as cooling would increase magma viscosity and form a constriction (Wylie et al., 1999), leading to increased strain rates.

CONCLUSIONS AND IMPLICATIONS

Tuffisite veins in a dissected rhyolitic conduit at Torfajökull, Iceland, are thought to record shallow, repeated fracture and healing of highly viscous magma. This process is attributed to non-Newtonian deformation of crystal-poor magma and is likely to be restricted to silicic compositions. Fracture events may generate seismic signals with similar magnitudes and repeat times to observed hybrid and long-period seismicity.

We emphasize the similarity between the deformed tuffisite veins described here and bands of discrete glass color and microlite content in obsidian. Trails of broken lithic fragments have been observed elsewhere parallel to similar flow banding in conduit-wall obsidian (Rust et al., 2003) and suggest that that particulate material may be incorporated into short-lived fractures in melt prior to such thorough welding that the melt phase is seemingly intact. A possible conclusion is that flow bands are textural records of earthquakes within silicic magma.

ACKNOWLEDGMENTS

Tuffen was supported by an Open University research studentship and the International Quality Network. We thank M. Ichihara, J. Neuberg, L. Wilson, B.F. Houghton, J. Taddeucci, and B. Kennedy for discussions and B.A. Chouet and K.V. Cashman for constructive reviews.

REFERENCES CITED

Chouet, B., 1988, Resonance of a fluid-driven crack—Radiation properties and implications for the source of long-period events and harmonic tremor: *Journal of Geophysical Research*, v. 93, p. 4375–4400.

Chouet, B.A., 1996, Long-period volcano seismicity: Its source and use in eruption forecasting: *Nature*, v. 380, p. 309–316.

Dingwell, D.B., 1996, Volcanic dilemma: Flow or blow?: *Science*, v. 273, p. 1054–1055.

Gil Cruz, F., and Chouet, B.A., 1997, Long-period events, the most characteristic seismicity accompanying the emplacement and extrusion of a lava dome in Galeras volcano, Colombia, in 1991: *Journal of Volcanology and Geothermal Research*, v. 77, p. 121–158.

Gomberg, J., 2001, The failure of earthquake failure

models: *Journal of Geophysical Research*, v. 106, p. 16,253–16,263.

Goto, A., 1998, A new model for volcanic earthquake at Unzen volcano: Melt rupture model: *Geophysical Research Letters*, v. 26, p. 2541–2544.

Gottsmann, J., and Dingwell, D.B., 2001, Cooling dynamics of spatter-fed phonolite obsidian flows on Tenerife, Canary Islands: *Journal of Volcanology and Geothermal Research*, v. 105, p. 323–342.

Gottsmann, J., and Dingwell, D.B., 2002, The thermal history of a spatter-fed lava flow: The 8-ka pantellerite flow of Mayor Island, New Zealand: *Bulletin of Volcanology*, v. 64, p. 410–422.

Gottsmann, J., Giordano, D., and Dingwell, D.B., 2002, Predicting shear viscosity during volcanic processes at the glass transition: A calorimetric calibration: *Earth and Planetary Science Letters*, v. 198, p. 417–427.

Hammer, J.E., Cashman, K.V., and Voight, B., 2000, Magmatic processes revealed by textural and compositional trends in Merapi dome lavas: *Journal of Volcanology and Geothermal Research*, v. 100, p. 165–192.

Heiken, G., Wohletz, K., and Eichelberger, J., 1988, Fracture fillings and intrusive pyroclasts, Inyo Domes, California: *Journal of Geophysical Research*, v. 93, p. 4335–4350.

Kumagai, H., and Chouet, B.A., 1997, Acoustic properties of a crack containing magmatic or hydrothermal fluids: *Journal of Geophysical Research*, v. 105, p. 25,493–25,512.

Lahr, J.C., Chouet, B.A., Stephens, C.D., Power, J.A., and Page, R.A., 1994, Earthquake classification, location, and error analysis in a volcanic environment: Implications for the magmatic system of the 1989–1990 eruptions at Redoubt Volcano, Alaska: *Journal of Volcanology and Geothermal Research*, v. 62, p. 137–151.

Marti, J., Soriano, C., and Dingwell, D.B., 1999, Tube pumices as strain markers of the ductile-brittle transition during magma fragmentation: *Nature*, v. 402, p. 651–653.

Maxwell, J.C., 1867, On the dynamical theory of gases: *Royal Society of London Philosophical Transactions*, v. 157, p. 49–88.

Neuberg, J., 2000, Characteristics and causes of shallow seismicity in andesite volcanoes: *Royal Society of London Philosophical Transactions*, ser. A, v. 358, p. 1533–1546.

Papale, P., 1999, Strain-induced magma fragmentation in explosive eruptions: *Nature*, v. 397, p. 425–428.

Romano, C., Mungall, J.E., Sharp, T., and Dingwell, D.B., 1996, Tensile strengths of hydrous vesicular glasses: An experimental study: *American Mineralogist*, v. 81, p. 1148–1154.

Rust, A.C., Manga, M., and Cashman, K.V., 2003, Determining flow type, shear rate and shear stress in magmas from bubble shapes and orientations: *Journal of Volcanology and Geothermal Research*, v. 122, p. 111–132.

Schwarzkopf, L.M., Schmincke, H.U., and Troll, V.R., 2002, Friction marks on blocks from pyroclastic flows at the Soufriere Hills volcano, Montserrat: Implications for flow mechanisms: *Comment: Geology*, v. 30, p. 190.

Shearer, P.M., 1999, Introduction to seismology: Cambridge, Cambridge University Press, 260 p.

Smith, J.V., 2002, Structural analysis of flow-related textures in lavas: *Earth-Science Reviews*, v. 57, p. 279–297.

Smith, J.V., Miyake, Y., and Oikawa, T., 2001, In-

terpretation of porosity in dacite lava domes as ductile-brittle failure textures: *Journal of Volcanology and Geothermal Research*, v. 112, p. 25–35.

Sparks, R.S.J., 1997, Causes and consequences of pressurization in lava dome eruptions: *Earth and Planetary Science Letters*, v. 150, p. 177–189.

Sparks, R.S.J., Tait, S.R., and Yanev, Y., 1999, Dense welding caused by volatile resorption: *Geological Society [London] Journal*, v. 156, p. 217–225.

Sparks, R.S.J., Murphy, M.D., Lejeune, A.M., Watts, R.B., Barclay, J., and Young, S.R., 2000, Control on the emplacement of the andesite lava dome of the Soufriere Hills volcano, Montserrat, by degassing-induced crystallization: *Terra Nova*, v. 12, p. 14–20.

Stasiuk, M.V., Barclay, J., Carroll, M.R., Jaupart, C., Ratte, J.C., Sparks, R.S.J., and Tait, S.R., 1996, Degassing during magma ascent in the Mule Creek vent (USA): *Bulletin of Volcanology*, v. 58, p. 117–130.

Tuffen, H., 2001, Subglacial rhyolite volcanism at Torfajökull, Iceland [Ph.D. thesis]: Milton Keynes, UK, Open University, 381 p.

Tuffen, H., McGarvie, D.W., Pinkerton, H., and Gilbert, J.S., 2003, Physical volcanology of a subglacial-to-emergent rhyolitic tuya at Raudufossafjöll, Torfajökull, Iceland: *Geological Society [London] Special Publication* 202, p. 213–236.

Uchida, N., and Sakai, T., 2002, Analysis of peculiar volcanic earthquakes at Satsuma-Iojima volcano: *Earth Planets Space*, v. 54, p. 197–209.

Umakoshi, K., Shimizu, H., Matsuwo, N., Matsushima, T., and Ohta, K., 1993, Seismic observations and infrared thermal surveys of the 1990–1993 eruption of Unzen volcano: *Journal of Natural Disaster Science*, v. 15, p. 63–77.

Voight, B., Sparks, R.S.J., Miller, A.D., Stewart, R.C., Hoblitt, R.P., Clarke, A., Ewart, J., Aspinall, W.P., Baptie, B., Calder, E.S., Cole, P., Druitt, T.H., Hartford, C., Herd, R.A., Jackson, P., Lejeune, A.M., Lockhart, A.B., Loughlin, S.C., Luckett, R., Lynch, L., Norton, G.E., Robertson, R., Watson, I.M., Watts, R., and Young, S.R., 1999, Magma flow instability and cyclic activity at Soufriere Hills volcano, Montserrat, British West Indies: *Science*, v. 283, p. 1138–1142.

Webb, S.L., and Dingwell, D.B., 1990, Non-Newtonian rheology of igneous melts at high stresses and strain rates—Experimental results for rhyolite, andesite, basalt, and nephelinite: *Journal of Geophysical Research*, v. 95, p. 15,695–15,701.

White, R.A., Miller, A.D., Lynch, L., and Power, J., 1998, Observations of hybrid seismic events at Soufriere Hills Volcano, Montserrat: July 1995 to September 1996: *Geophysical Research Letters*, v. 25, p. 3657–3660.

Wilding, M., Dingwell, D., Batiza, R., and Wilson, L., 2000, Cooling rates of hyaloclastites: Applications of relaxation geospeedometry to undersea volcanic deposits: *Bulletin of Volcanology*, v. 61, p. 527–536.

Wylie, J.J., Helfrich, K.R., Dade, B., Lister, J.R., and Salzig, J.F., 1999, Flow localization in fissure eruptions: *Bulletin of Volcanology*, v. 60, p. 432–440.

Manuscript received 25 April 2003

Revised manuscript received 26 June 2003

Manuscript accepted 14 August 2003

Printed in USA